

**Portsaid University,
Faculty of Science,
Department of Physics.**



Photovoltaic properties of organic semiconductor material

NAME:Areeg Belal Hassan

Supervisor:Dr_Eman EL_esh

Contents

Chapter1

1.1 The history highlight of solar cells	6
1.2 Organic Semiconductor	15
1.2.1 The bonding of sp_2-hybridised carbon	16
1.2.2 Small-molecule organic semiconductors	18
1.2.3 Organic Semiconductor Devices	19
1.2.4 Organic Photovoltaic (OPV) and Quantum Dots	21
1.3 Structure of a Solar Cell	23
1.3.1 A typical solar cell is a multi-layered material	23
1.3.2 The basic steps in the operation of a solar cell	25
1.4 Types of Solar Cells	27
1.5 The conduction mechanism of p-n junction	30
1.6 Solar cell output parameters	37
1.7 Experimental Techniques and Methods of Calculations	40
1.7.1 Au/CuTPP/p-Si/Al Heterojunction	40
1.7.1.1 Devices preparation	40

1.7.2 Current-Voltage (I-V) measurements	41
1.7.3 Capacitance-Voltage (C-V) measurements	42
Chapter2	
2.1CuTPP/p-Si Organic-Inorganic Photovoltaic Cells	44
2.1.1 Dark Current-Voltage Characteristics	44
2.2 Photovoltaic Properties	51
Conclusion	54
Reference	55

All gratitude is due to ALLAH who guided me and gave me strength and patience to execute this Essay.

My soul thanks to Dr. Eman El-esh for suggesting the point of research, supervising, revising for preparation this Essay.

I would like to sincerely thank Prof. Dr. Mossad El-Metwally for instructing me to the way and learning me a lot. All my thanks to Prof. Dr. Waleed Moslem and Prof. Dr. Abd El-Raouf for learning me a lot.

I would like to thank all my doctors' lecturer in my faculty beloved of science of Port Said, Physics Department for their help. The brotherly feeling to all friends and colleagues.

CHAPTER1

1.1 The history highlight of solar cells (photovoltaic cells):

A photoelectric cell which designed to convert sunlight into electrical energy, typically consisting of layers or sheets of specially prepared silicon is called a solar cell. Electrons displaced through the photoelectric effect by the Sun's radiant energy in one layer, flow across a junction to the other layer, creating a voltage across the layers that can provide power to an external circuit. Solar cells are used as power supplies in calculators, satellites, and other devices, and as a primary source of electricity in remote locations [1].

In 1839 – The photovoltaic effect was discovered by Alexandre-Edmond Becquerel, who was a French physicist. This was “the beginning” of the solar cell technology. Becquerel's experiment was done by illuminating two electrodes with different types of light. The electrodes were coated by light sensitive materials, AgCl or AgBr, and carried out in a black box surrounded by an acid solution. The electricity increased when the light intensity increased [2].

In 1873 – The photo conductivity of an element, selenium, was discovered by Willoughby Smith, who was an English electrical engineer [2].

In 1876 – Selenium produces electrical current when it is exposed to sun light. William Grylls Adams and Richard Evans Day proved that it is possible to convert solar energy into electricity directly, without any moving parts or heat. The solar cell was very inefficient, and it couldn't be used to run any electrical equipment [2].

In 1904 – A German physicist, Wilhelm Ludwig Franz Hallwachs, discovered that a combination of copper and cuprous oxide was photosensitive [2].

In 1905 – Albert Einstein published his paper about the photoelectric effect. There he claimed that light consists of “packets” or quanta of energy, which we now call photons. This energy varies only with its frequency (electromagnetic waves, or the “color of the light”). This theory was very simple, but revolutionary, and it explained very well the absorption of the photons regarding to the frequency of the light [2].

In 1916 – Robert Andrews Millikan provided experimental proof of the photoelectric effect. He was an American experimental physicist who later won the Nobel Prize for his work on the photoelectric effect and for his measurement of the charge of the electron [2].

In 1918 – Jan Czochralski, a Polish chemist, developed a way to grow single-crystal silicon. This increased the efficiency of the silicon-based cells considerably [2].

In 1923 – Albert Einstein received the Nobel Prize for his theories explaining the photoelectric effect, which he published 18 years earlier [2].

In 1930 – Walter Schottky, Neville Mott and some others developed a theory of metal-semiconductor barrier layers [2].

In 1953 – Dr. Dan Trivich of Wayne State University makes the first theoretical calculations of the efficiencies of various materials of different band-gap widths based on the spectrum of the sun [2].

In 1954 – Three researchers, Gerald Pearson, Daryl Chapin and Calvin Fuller, at Bell Laboratories discovered a silicon solar cell, which was the first material to directly convert enough sunlight into electricity to run electrical devices. The efficiency of the silicon solar cell, which Bell Labs produced, were 4%, which later increased to 11%. The cells were made by hand and cost \$1000 per watt [2].

In 1958 – The first PV-powered satellite, Vanguard I, was launched. The solar panel had an area of 100cm² and delivered an effect of approximately 0.1W. The satellite power system operated for 8 years, and is the world's oldest satellite still in orbit (2007) [2].

In 1959 – Hoffman Electronics achieved 10% efficient commercially available PV cells and demonstrated the use of a grid contact to significantly reduce series resistance[2].

In 1959 – Explorer-6 was launched with a PV array of 9600 cells, each only 1 cm x 2 cm [2].

In 1960 – Hoffman Electronics achieved 14% efficient PV cells [2].

In 1970 – First highly effective GaAs heterostructure solar cells are created by Zhores Alferov (a Russian physicist) and his team in the USSR [2].

In 1972 – The Institute of Energy Conversion is established at the University of Delaware to perform research and development on thin-film photovoltaic and solar thermal systems, becoming the world's first laboratory dedicated to photovoltaic research and development [2].

In 1976 – David Carlson and Christopher Wronski of RCA Laboratories produced the first amorphous silicon photovoltaic cells, which could be less expensive to manufacture than crystalline silicon devices. The efficiency was of 1.1% [2].

In 1981 – Paul MacCready builds the first solar-powered aircraft, the Solar Challenger, and flies it from France to England across the English Channel. The aircraft had over 16,000 solar cells mounted on its wings, which produced a power of 3kW [2].

In 1982 – Hans Tholstrup, an Australian, drives the first solar-powered car, the Quiet Achiever, 4,000km between Sydney and Perth in 20 days. That was 10 days faster than the first gasoline-powered car to do so. The maximum speed was 72 km/h, and the average speed was 24 km/h [2].

In 1985 – The University of South Wales breaks the 20% efficiency barrier for silicon solar cells under one sun conditions [2].

In 1989 – Reflective solar concentrators are first used with solar cells [2].

In 1989 – studied the electrical conductivities for metallo porphyrin complexes where the metal is Co, Cu and Zn. the temperature dependence of the electrical conductivities to estimate the activation energy for each complex [3].

In 1991 – Efficient Photoelectrochemical cells (PEC) are developed. Each cell consists of a semiconducting photoanode and a metal cathode immersed in an electrolyte.

The Dye-sensitized solar cell (DSC), also called Grätzel cells, is invented. It was a new class of low-class DSC [2].

In 1992 – University of South Florida develops a 15.9% efficient thin-film photovoltaic cell made of cadmium telluride, breaking the 15% barrier for the first time for this technology [2].

In 1994 – The National Renewable Energy Laboratory develops a solar cell, made from gallium indium phosphide and gallium arsenide, that becomes the first one to exceed 30% conversion efficiency [2].

In 1999 – Spectrolab, Inc. and the National Renewable Energy Laboratory develops a photovoltaic solar cell that converts 32.3 percent of the sunlight that hits it into electricity. The high conversion efficiency was achieved by combining three layers of photovoltaic materials into a single solar cell. The cell performed most efficiently when it received sunlight concentrated to 50 times normal. To use such cells in practical applications, the cell is mounted in a device that uses lenses or mirrors to concentrate sunlight onto the cell.

Such “concentrator” systems are mounted on tracking systems that keep them pointed toward the sun[2].

In 2000 – Two new thin-film solar modules, developed by BP Solarex, break previous performance records. The company’s 0.5-square-meter module achieves 10.8 % conversion efficiency—the highest in the world for thin-film modules of its kind. And its 0.9-square-meter module achieved 10.6% conversion efficiency and a power output of 91.5 watts — the highest power output for any thin-film module in the world [2].

In 2002 – reported that organic electronic materials are of interest for future applications in solar cells although results for single layer organic materials have been disappointing, high photocurrent efficiencies can be achieved in composite systems including both electron donating and electron accepting components .These problems are being tackled by synthesis of new materials, the use of new material combinations, and optimization of

molecular design and processing conditions to control morphology [4].

In 2008 – constructed a heterojunction device of Au/FeTPP/n-Si/Al by thermal evaporation technique. Results showed a rectification behavior. The Au/Fe-TPP/n-Si/Al device indicates a photovoltaic behavior with an open circuit voltage V_{oc} of 0.52 V, short circuit current I_{sc} of 2.22×10^{-6} A, fill factor FF of 0.49 and conversion efficiency 1.13% under white light illumination of power 50 W/m [5].

In 2011 – constructed heterojunction solar cell as Au/TPP/n-Si/Al using thermal evaporation technique. The C-V measurements showed that the diode is linearly graded junction and the width of depletion layer and built in voltage were estimated. I-V characteristic and photovoltaic properties under illumination have also been investigated of Au/TPP/n-Si/Al solar cell were evaluated[6,7].

In 2011 – studied transport mechanisms of ZnTPP. The C-V measurements on Au/ZnTPP/n-si/Al showed that

the formed junction is linearly graded one. A hybrid solar cell of Au/ZnTPP/n-si/Al had been constructed by growing ZnTPP film via thermal evaporation technique on n-Si wafer. Dark I-V measurements of the device at different temperatures showed that there are three conduction mechanisms operating in the device. The dominance of any of them depends on applied potential [8].

In 2011 – prepared thermally-evaporated thin films of tetraphenyl porphyrin, TPP, It was found that the DC conductivity increases with increasing temperature and film thickness .It had been shown that theoretical curves generated from correlated barrier hopping (CBH) model gives the best fitting with experimental results. Analysis of these results proved that conduction occurs at low temperatures (300-370) K [9].

1.2 Organic Semiconductor:

Organic semiconductors are easy to process and can be used to make devices that are transparent, flexible and cheap. However, they are also fragile and not particularly good at conducting electricity. Three papers in the October

2009 issue of Nature Nanotechnology show that careful processing can redress these drawbacks, without compromising those qualities that make organics attractive in the first place [10].

1.2.1 The bonding of sp_2 -hybridised carbon:

Organics Semiconductors are based on the unusual properties of the carbon atom: Among other configurations, it can form the so-called sp_2 -hybridisations where the sp_2 -orbitals form a triangle within a plane and the p_z -orbitals are in the plane perpendicular to it.

S-bond between two carbons can then be formed by formation of an orbital overlap of two sp_2 -orbitals. The energy difference between the occupied binding orbitals and the unoccupied anti-binding orbitals is quite large and well beyond the visible spectral range. Correspondingly, longer chains of bound carbon atoms would have a large gap between the highest occupied molecular orbital (HOMO) and the lowest unoccupied molecular orbital (LUMO), leading to insulating properties.

However, in the sp_2 -hybridisation, the p_z -orbitals form additionally π -bonds. These bonds have much smaller energetic difference between the HOMO and LUMO, leading to strong absorption in or near the visible spectral range and to semiconducting properties [10].

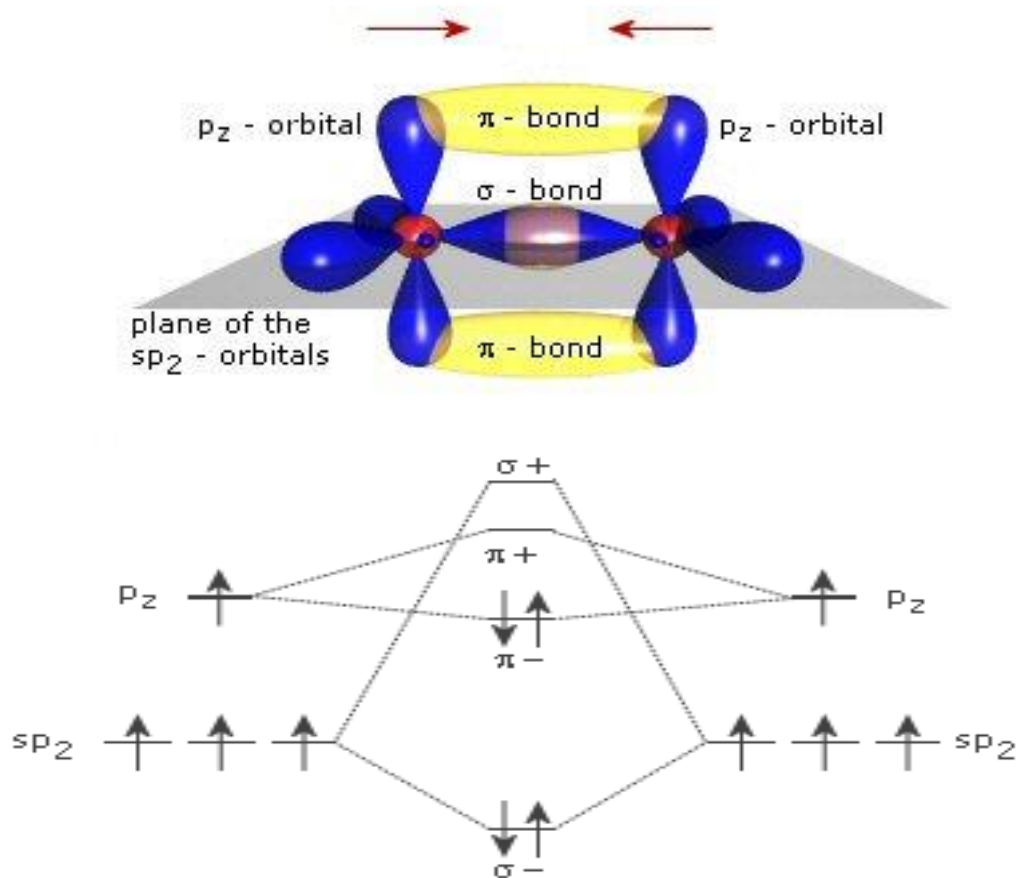


Fig. (1.1): Scheme of the orbitals and bonds for two sp_2 -hybridised carbon atoms.

1.2.2 Small-molecule organic semiconductors:

If carbon atoms form larger molecules, typically with benzene rings as the basic unit, the p-bonds become delocalized and form a p-system which often has the extensions of the molecule. The gap between occupied and empty states in these p-systems becomes smaller with increasing delocalization, leading to absorption and fluorescence in the visible. These substances can be prepared as molecular single crystals. Due to the close coupling of the p -systems of the molecules in these crystals, they show in a purified form remarkable transport properties, including band transport up to room temperature with mobilities of 1-10 cm²/Vs. Most of the molecules can also be easily evaporated to form polycrystalline (hopping transport with mobilities typically around 10⁻³ cm²/Vs at 300K) or amorphous (hopping with mobilities typically around 10⁻⁵ cm²/Vs at 300K) layers[10].

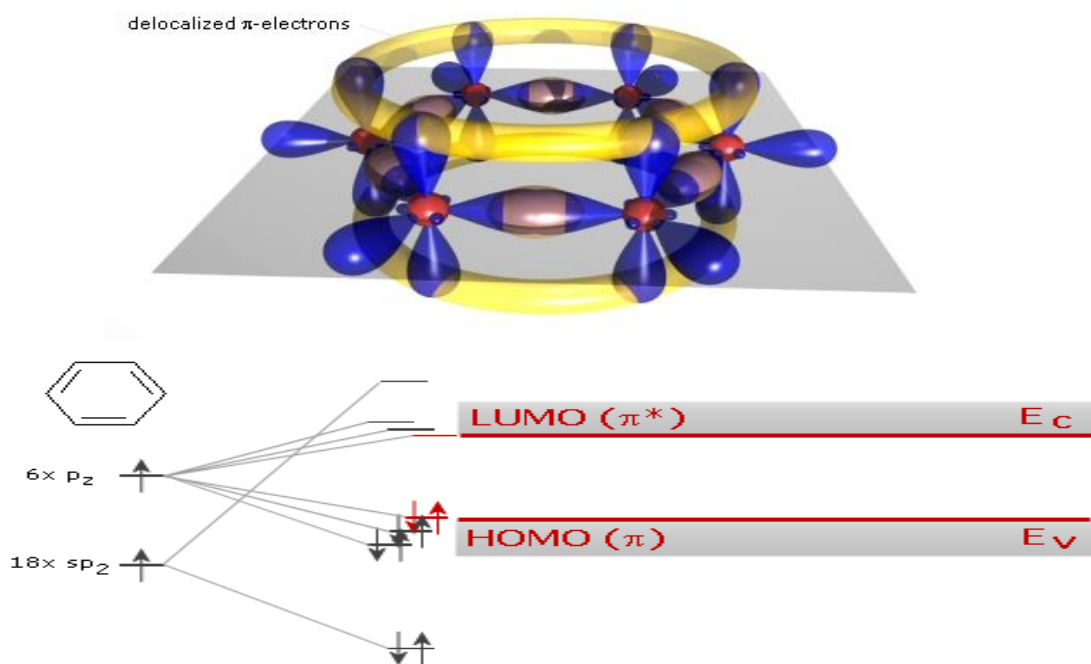


Fig. (1.2): Scheme of a benzene ring (top) and the energy structure of small-molecule organics.

1.2.3 Organic Semiconductor Devices :

Organic semiconductor refers to organic (non-metallic) materials that exhibit semiconductor properties. Semi conductivity in these materials occurs for single molecules, short chains of molecules and long polymer chains depending on the material. Small molecule semiconductors include pentacene, rubrene and anthracene, as well as larger molecules such as fullerenes and fullerene derivatives [11].

The drive to produce such devices comes from advantages afforded by these materials over traditional silicon-based semiconductor devices. Most organic materials are much less expensive to generate than highly crystalline inorganic semiconductors, and also may be used to make devices with inexpensive fabrication methods. In particular, most organics are soluble in one or more common solvents - this allows for the possibility of solution processing which can produce many devices at a fraction of the cost. Additionally, most devices require an annealing step to reach high performance that is generally at high temperatures (at least 500 °C for silicon), but is much less or not required for organic materials. The low annealing temperature of organics allows for flexibility of substrate choice for organic devices such as transparent plastics that could not withstand the high annealing temperature of silicon [11].

1.2.4 Organic Photovoltaic (OPV) and Quantum Dots:

Organic photovoltaic cells are solar cells that utilize organic polymers and small molecules as the active layer for light absorption and charge transport. A solar cell functions through the use of a semiconductor layer with a bandgap of suitable size. When light is incident on the semiconductor (1), photons may be absorbed by electrons in valence orbitals of the semiconductor. These electrons are then excited to conduction orbitals (3), leaving holes behind in the valence band (2) creating a charge carrier pair or exciton. Solar cells are designed using a p-n junction with both n and p-type materials such that the free holes and electrons flow in opposite directions, producing a direct current (4) as shown in Fig. (1.3). Holes flow through the p-type material and electrons through the n-type such that recombination is minimized. Recombination occurs when a conduction electron and a hole collide, annihilating the hole and returning the electron to the valence band. This is undesirable for the efficiency of the solar cell as only free charge carriers contribute to the current[11].

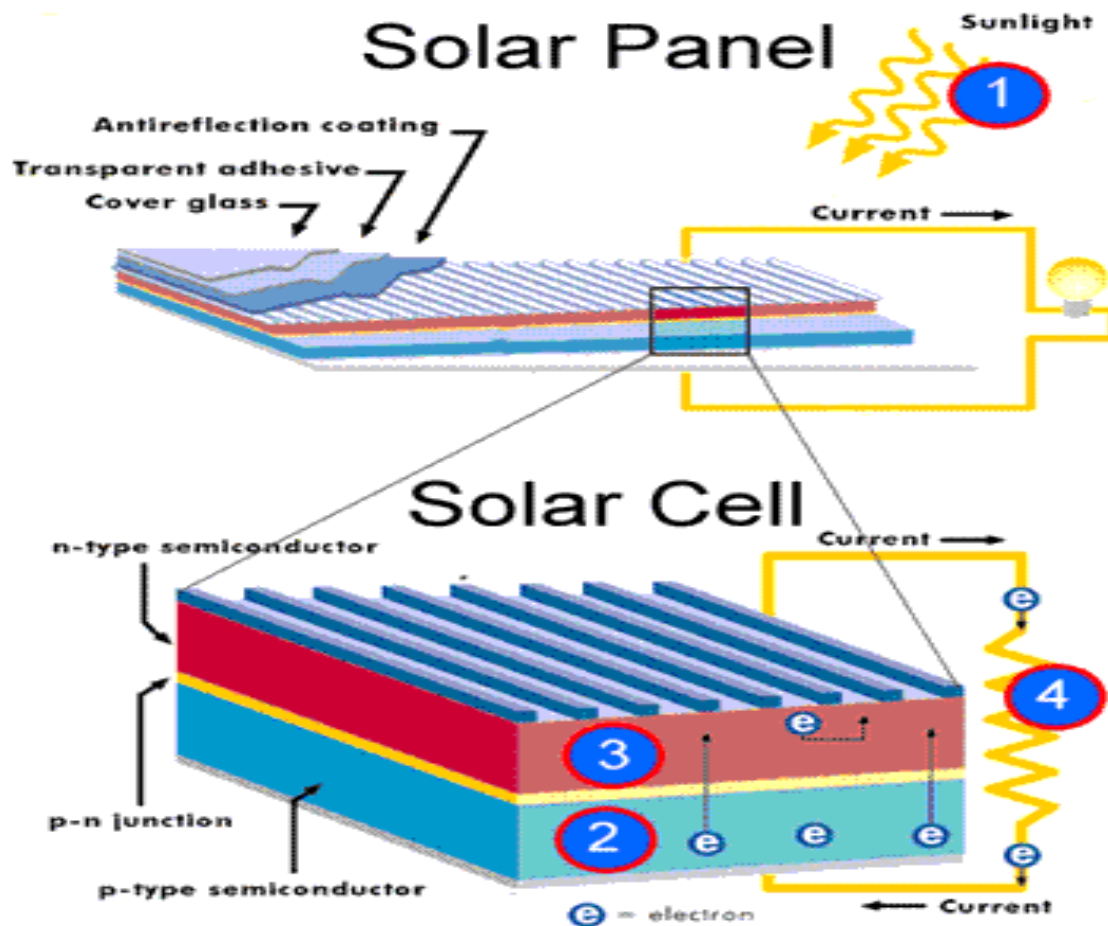


Fig. (1.3) organic photovoltaic cell

When using organic materials as the active layer, there are a number of advantages and disadvantages. Organic materials are easy to process into large area solar cells at a comparatively low cost due to their structure being generally self-organized polycrystalline. However, this polycrystalline nature typically also results in low energy conversion efficiency compared to inorganic solar cells. Inorganic cells made from materials such as silicon

are expensive to produce as they have highly crystalline structures which result in high efficiency. OPV research therefore concentrates on improving efficiency by optimizing such parameters as effective charge separation (increased exciton diffusion length), charge mobility, crystal structure and minimizing impurities. Organics are also more sensitive to oxidation effects and temperature variations which can cause decreased performance over time[11].

1.3 Structure of a Solar Cell:

1.3.1 A typical solar cell is a multi-layered material:

Let's review what the layers are:

Cover Glass - this is a clear glass layer that provides outer protection from the elements.

- Transparent Adhesive - this holds the glass to the rest of the solar cell.
- Anti-reflective Coating - this substance is designed to prevent the light that strikes the cell from bouncing off so that the maximum energy is absorbed into the cell.

- Front Contact - transmits the electric current.
- N-Type Semiconductor Layer - This is a thin layer of silicon which has been doped with phosphorous.
- P-Type Semiconductor Layer - This is a thin layer of silicon which has been doped with boron.
- Back Contact - transmits the electric current [12].

A solar cell is an electronic device which directly converts sunlight into electricity. Light shining on the solar cell produces both a current and a voltage to generate electric power. This process requires firstly, a material in which the absorption of light raises an electron to a higher energy state, and secondly, the movement of this higher energy electron from the solar cell into an external circuit. The electron then dissipates its energy in the external circuit and returns to the solar cell. A variety of materials and processes can potentially satisfy the requirements for photovoltaic energy conversion, but in practice nearly all photovoltaic energy conversion uses semiconductor materials in the form of a p-n junction[13].

1.3.2 The basic steps in the operation of a solar cell are:

- the generation of light-generated carriers;
- the collection of the light-generated carries to generate a current;
- the generation of a large voltage across the solar cell; and
- the dissipation of power in the load and in parasitic resistances[12].

Solar cells are composed of various semiconducting materials. Semiconductors are materials, which become electrically conductive when supplied with light or heat, but which operate as insulators at low temperatures.

Over 95% of all the solar cells produced worldwide are composed of the semiconductor material Silicon (Si). As the second most abundant element in earth's crust, silicon has the advantage, of being available in sufficient quantities, and additionally processing the material does not burden the environment. To produce a solar cell, the semiconductor is contaminated or "doped". "Doping" is

the intentional introduction of chemical elements, with which one can obtain a surplus of either positive charge carriers (p-conducting semiconductor layer) or negative charge carriers (n-conducting semiconductor layer) from the semiconductor material. If two differently contaminated semiconductor layers are combined, then a so-called p-n-junction results on the boundary of the layers as shown in Fig. (1.4) [11].

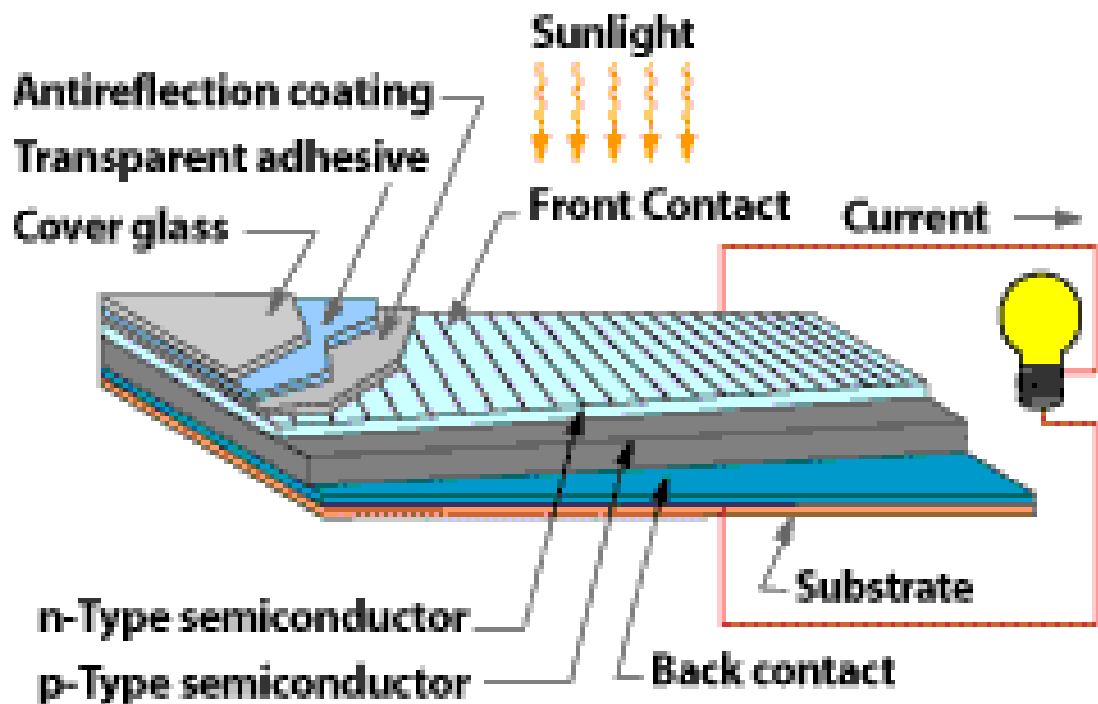


Fig. (1.4) structure of solar cell.

1.4 Types of Solar Cells:

Because of the extensive research being done on solar energy there are now many types of solar cells on the market. All of them follow the principles described when it comes to generating an electric current. However, many different approaches are now used to create the structures in order to reduce the costs of production. These approaches involve a tradeoff between lower manufacturing costs versus lower efficiency in converting sunlight to electricity. The three most common approaches are summarized below:

- Monocrystalline Silicon - This type of solar cell uses a single layer of silicon for the semi-conductor. In order to produce this type of silicon it must be extremely pure which means it is the most expensive type of solar cell to produce.
- Polycrystalline Silicon to make polycrystalline silicon cells liquid silicon is poured into blocks that are subsequently sawed into plates. This type of approach produces some degree of degradation of the silicon

crystals which makes them less efficient. However, this type of approach is easier and cheaper to manufacture.

- Amorphous Thin Film Silicon - This type of solar cell uses layers of semiconductor that are only a few micrometers thick (about 1/100th the thickness of a human hair). This lowers the material cost but makes it even less efficient than the other types of silicon. However, because it is so thin this type of cell has the advantage that it can be placed on a wide variety of flexible materials in order to make things like solar shingles or roof tiles[13].

Another way of looking at solar cells is in terms of the types of materials they are made with. While silicon is the most commonly used crystal a number of other materials can be used as well. These include the following:

- gallium arsenide
- copper indium diselenide
- cadmium telluride

Different types of substances perform better under certain light conditions. Some cells perform better outdoors (i.e., optimized for sunlight), while others perform better indoors (optimized for fluorescent light)[13].

Material	Level of efficiency % in Lab	Level of efficiency % in Production
Monocrystalline Silicon	approx. 24	14 to17
Polycrystalline Silicon	approx. 18	13 to15
Amorphous Silicon	approx. 13	5 to7

1.5 The conduction mechanism of p-n junction:

There are two effects in real diodes due to charge storage mechanisms.

The first charge storage mechanism is charge storage in the depletion region of the p-n junction and the second one is in the neutral regions adjacent to the depletion region. The capacitance associated with the p-n junction depletion region is called junction capacitance and is in parallel with the ideal diode. So, the dynamic capacitance-voltage (C-V) characteristics are very important beside the static current-voltage (I-V) characteristics to determine several electrical parameters and provide a good investigation for the diode.

I-V characteristic shows the relationship between the current through an electronic device and the applied voltages across its terminals. It is used as a critical tool to determine the basic parameters of a device and to model its behavior in an electrical circuit. I-V characteristics of metal/semiconductor/metal devices are controlled by two basic processes: (a) injection of charge carriers from

electrodes into the semiconductor layer; and (b) transport of charge carriers in the bulk of the film. The current is then either injection limited or bulk transport limited due to mismatch of energy levels between the electrode work function and the corresponding transport levels of the semiconductor and an intrinsic mobility of the bulk or a charge trapping, respectively. Some conduction mechanisms of metals/semiconductor contacts are:

A- Ohmic mechanism:

Ohmic mechanism is defined as an infinite reservoir of charge that is able to sustain a steady state space charge limited current (SCLC) in a device. The current-voltage relation is often linear at low bias up to a certain value since the electric field due to the injected carriers is negligible compared to that due to the applied bias. The slope of a log-log plot between the current and the voltage at low voltages is then equal to 1, and the behaviour is described by Ohm's law, as, [14].

$$J_{Ohm} = qn^g \mu \frac{V}{d} \quad (1.1)$$

Where q is the electronic charge, n^g is the charge carrier, μ is the carrier mobility, V is the applied voltage and d is the thickness of the sample.

B- Space -Charge -Limited Currents (SCLC):

Space charge limited conductivity (SCLC) is undoubtedly the most important conduction process in organic thin films, having been observed in many different materials. SCLC occurs only when the injecting electrode is an ohmic contact and therefore a reservoir of charge is available. These results have lent greater support to the use of the techniques of Space-charge-limited currents (SCLC) to determine properties of trap states which is located in the forbidden gap of many materials [15].

The first indication of Space charge limited current in the organic semiconductors was the work of Heilmeier and Warfield on single crystals of metal-free phthalocyanine in the dark and under illumination conditions[16].

When ohmic contacts are applied majority carriers may be injected into the material, and when the injected

carrier concentration exceeds that of the thermally generated concentration the SCLC current becomes dominant. It occurs when the transit time of any excess injected carriers is less than the bulk dielectric relaxation time. Under these circumstances, The space charge limited current takes the simple form of Child's law [17].

This behavior is characterized by a strict quadratic dependence of current on voltage (slope \approx 2 in a logJ-logV plot)

$$J_{SCLC} = \frac{9}{8} \varepsilon_0 \varepsilon_r \mu \frac{V^2}{d^3} \quad (1.2)$$

where ε_r is the relative permittivity of the material, ε_0 is the permittivity of free space. If the traps are shallow and located at a discrete energy E, above the valence band edge, the SCLC is given by[18]:

$$J_{SCLC} = \frac{9}{8} \varepsilon_0 \varepsilon_r \theta' \mu \frac{V^2}{d^3} \quad (1.3)$$

where θ' is trapping factor.

It is clear that there is a transition voltage between the two conduction mechanisms described by equation (1.3), which occurs at a transitional voltage V_t , when the injected carrier concentration first exceeds the thermally generated carrier concentration. This voltage has the following expression.

$$V_t \approx \frac{q p_o d^{*2}}{\epsilon_r \epsilon_o} \quad (1.4)$$

Where p_o is the hole occupancy (i.e. the concentration of traps not occupied by electrons) of the traps in the active region of the diode and d^* is the thickness of the active region.

C- Thermionic emission mechanism:

At low electrical fields when the slope of $\ln(J)$ versus $\ln(V)$ is about 1, the region is considered as being ohmic. Above the ohmic region, the current-voltage characteristics may be fitted to the Richardson–Schottky (RS) Emission model [19].

The essential assumption of the RS model of thermionic emission is that an electron from the metal can be injected into the semiconductor, once it has acquired a thermal energy sufficient to cross the maximum potential. The current density is given by [19]:

$$J = A^* T^2 \exp\left(-\frac{\phi_{b0}}{k_B T}\right) \quad (1.5)$$

where ϕ_{b0} is the barrier height and A^* is the Richardson–Schottky constant ($A^* = 120A/cm^2K$) for free electron, where the effective mass m^* equals that of the free electron. According to above equation, plots of $\ln\left(\frac{J}{T^2}\right)$ versus $1000/T$ is straight line, ϕ_{b0} and A^* can be determined from the slope and the intercept of the line respectively. This model usually valid only at lower fields and at higher temperatures.

At higher fields, the metal work function for thermionic emission is reduced, thus lowering the Schottky barrier height. The Schottky equation may be written as, [20].

$$J = A^* T^2 \exp\left(-\frac{\phi_{b0}}{k_B T}\right) \exp\left[\left(\frac{e^3 V}{4\pi\epsilon_o \epsilon_r d}\right)^{1/2} / k_B T\right] \quad (1.6)$$

where the applied voltage V is positive for forward bias and negative for reverse bias. Equation (1.6) may be rewritten as

$$\ln\left(\frac{J}{T^2}\right) = \ln(A^*) + \left[\left(-\phi_{b0} + \sqrt{\frac{e^3 V}{4\pi\epsilon_o \epsilon_r d}} \right) \cdot \frac{1}{k_B} \right] \cdot \frac{1}{T} \quad (1.7)$$

According to equation (1.7), plots of $\ln\left(\frac{J}{T^2}\right)$ versus $1000/T$ are straight lines, since all the other parameters are constant, at a given voltage V. The expression in the square brackets of equation (1.7) represents the slope and is called activation energy. The effective barrier height between the electrode and the film may be calculated from the slope, thus,

$$\phi_{b0} = \left(-k_B \times slope + \sqrt{\frac{e^3 V}{4\pi\epsilon_o \epsilon_r d}} \right). \quad (1.8)$$

E- Direct tunneling mechanism:

Direct tunneling is a simple tunneling mechanism, which is more appropriate only at low-bias voltage range. In this model, the localized charges move through the lattice via successive transitions from one site to the other. A charge carrier may tunnel through the energy barrier between adjacent sites. The current density, J , a cross junction is given by [21]:

$$J = V \cdot \exp\left(-\frac{2l}{h} \sqrt{2m\phi_{b0}}\right) \quad (1.9)$$

where ϕ_{b0} and l are barrier height and width respectively. Above equation predicts that this model does not have temperature-dependent J–V behavior.

1.6 Solar cell output parameters:

Three parameters are usually used to characterize solar cell outputs.

A- The short – circuit current, I_{sc} :

The I_{sc} is the maximum current the solar cell can put out under a given illumination power without an external

voltage source connected. The current is dependent upon the formation of excitons via light absorption, dissociation of the exciton at the donor-acceptor heterojunction interface, and finally the collection of the free charges at the electrodes. The charge collection efficiency is assumed to be close to 100% because of the presence of the built-in electric field. Because of the close to 100% efficiency for this process it is clear that increasing the I_{sc} will not be accomplished with this process. The exciton dissociation process is also assumed to be approximately 100% efficient, meaning all excitons that reach the donor-acceptor heterojunction interface dissociate into free electrons and free holes. This is assumed because the charge transfer process is so much faster than any other competing process [22, 23].

B- Fill Factor, FF:

The fill factor is an indication of the quality of the diode and the squareness of the J-V curve. The FF is known to be directly related to the resistance in the device [16]. There are generally two types of resistance that can be

present in the cell that would have an effect on the FF. The first is the parallel or shunt resistance. It arises from leakage of current through the device and leakage at the edges of the device. Poorly rectifying devices are attributed mainly to shunt resistance. The second type of resistance that can lead to problems and show itself by decreasing the FF is series resistance.

C- Open-Circuit Voltage, V_{oc} :

The final parameter to be examined is V_{oc} . V_{oc} is the maximum voltage a solar cell can put out. It is measured by connecting the illumination solar cell to voltmeter.

More recently it has been suggested in the polymer solar cell community that the V_{oc} is highly influenced by the energy difference between the HOMO of the donor-like material and the LUMO of the acceptor-like material [24, 25].

1.7 Experimental Techniques and Methods of Calculations:

1.7.1 Au/CuTPP/p-Si/Al Heterojunction:

1.7.1.1 Devices preparation:

Au/CuTPP/p-Si/Al heterojunction was prepared by using a polished and etched p-type single crystal silicon wafer with a thickness of 400 μm and area 2.2 cm^2 . The wafer was rinsed successively in distilled water for some time to remove any dust particles, followed by ethyl alcohol to remove any grease material and then washed in distilled water. The silicon wafer was etched using CP_4 etching solution for 1.5 min, etching solution was prepared by adding 18 ml of HF to 1.5 ml of acetic acid and 57 ml Conc. HNO_3 . After etching, the silicon wafer was washed for two minutes by distilled water and then by ethyl alcohol. Then the silicon wafer was coated from one side by aluminum electrode while the other side was coated by CuTPP thin film with thickness 100 nm and the other masked electrode Au was deposited onto CuTPP thin film as ohmic contact[26].

The Au/CuTPP/p-Si/Al solar cell schematic diagram is shown in Fig.(1.5).

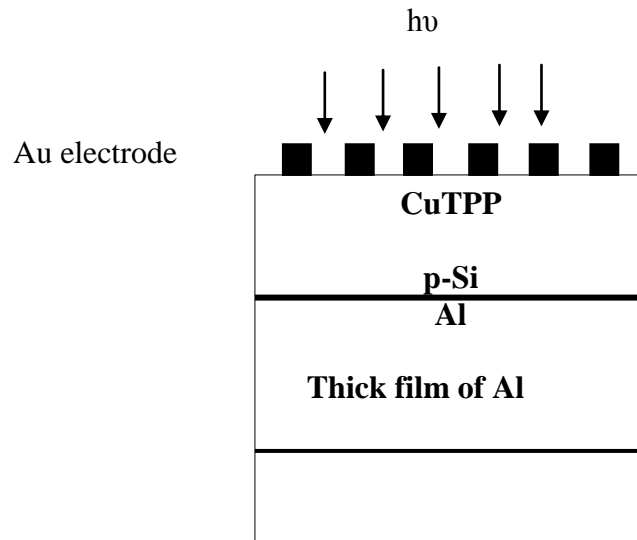


Fig.(1.5) Schematic diagram of Au/CuTPP/p-Si/Al solar cell

1.7.2 Current-Voltage (I-V) measurements:

The dark current-voltage (I-V) characteristics of Au/CuTPP/p-Si/Al heterojunction diode at different temperatures, ranged from 293 to 353 K with step of 20 K ,were measured by using a high impedance Keithley electrometers(model 617).

The illuminated current–voltage characteristics of Au/CuTPP/p-Si/Al heterojunction diode were also measured using the circuit illustrated in Fig.1-6.

The incident white light provided by halogen lamp of intensity $5\text{mW}/\text{cm}^2$, falls normally through the gold window on the organic film. The intensity of the incident light is recorded by a digital light meter (Lutro-Model LX-107).

1.7.3 Capacitance-Voltage (C-V) measurements:

The capacitance-voltage (C-V) characteristics of fabricated Au/CuTPP/p-Si/Al heterojunction diode were measured at room temperature at 1MHz using a computerized capacitance-voltage system, consisting of C-V meter (Model 4108) in air and at dark conditions, interfaced to a personal computer.

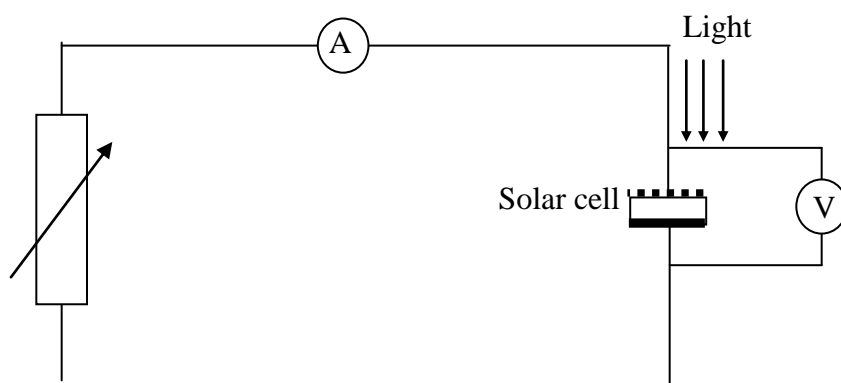


Fig.(1.6) Electric circuit for measuring current-voltage characteristic of Au/CuTPP/p-Si/Al heterojunction under illumination.

CHAPTER2

2.1 CuTPP/p-Si Organic-Inorganic Photovoltaic Cells:

2.1.1 Dark Current-Voltage Characteristics:

Fig.2-1 shows a semi logarithmic plot of the forward and reverse currents versus the applied voltage of Au/CuTPP/p-Si/Al heterojunction diode in the temperature range 293–353 K.

The values of the current increases as the temperature increase.

The heterojunction exhibits rectification behavior showing a diode-like characteristic. The specific parameters of the junction such as the diode quality factor (m), the rectification ratio (RR), the series resistance (R_s), the shunt resistance (R_{sh}), the barrier height at the interface of the junction (ϕ_{b0}) can be estimated from I-V characteristics curve.

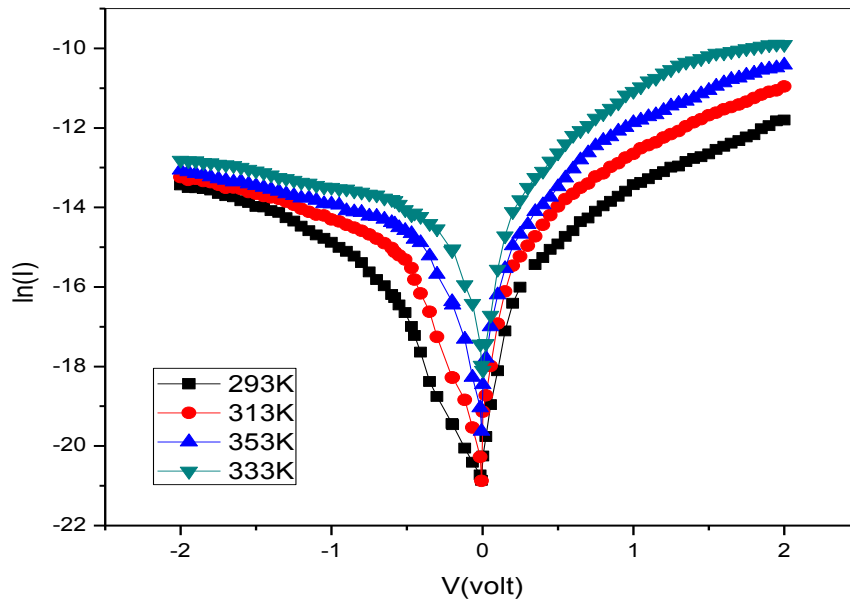


Fig.2-1 I-V characteristic of Au/CuTPP/p-Si/Al device in the dark at different temperature in forward and reverse bias.

The maximum rectification ratio is observed at $\pm 0.25V$ at room temperature condition as shown in

Fig.2-2.

The junction resistance, R_j of Au/CuTPP/p-Si/Al heterojunction device is determined from I-V characteristic curves according to following formula[27]:

$$R_j = \frac{\partial V}{\partial I} \quad (2.1)$$

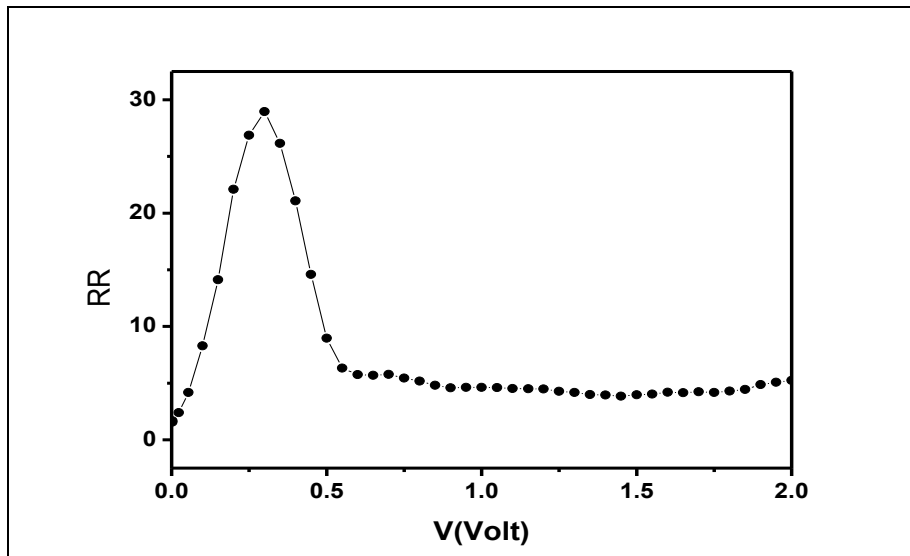


Fig.2-2 Relation between the rectification ratio, RR, and the bias potential for Au/CuTPP/p-Si/Al heterojunction diode.

The dark current-voltage characteristics are extremely useful in identifying the operating transport conduction mechanisms.

Fig.2-3 shows the current-voltage (I-V) characteristic observed for the heterojunction device under the forward bias at different temperatures. For each curve; there are two distinct voltage regions indicating presence of two different predominant conduction mechanisms.

In the first low voltage region $0 < V < 0.2$ Volt; the relation between $\ln(I)$ versus V is linear and the current of

the Au/CuTPP/p-Si/Al device obeys the thermoionic emission of holes from p-Si substrate over the organic/inorganic barrier in the device. The diode current expression for this conduction mechanism is given by [28].

$$I = I_{01} \left(\exp \left(\frac{qV}{m_1 k_B T} \right) - 1 \right) \quad (2.2)$$

Where q is the electric charge, k_B the Boltzmann's constant, T the absolute temperature and m_1 is the ideality factor which is determined from the slope of the linear region of the forward bias $\ln(I)$ - V .

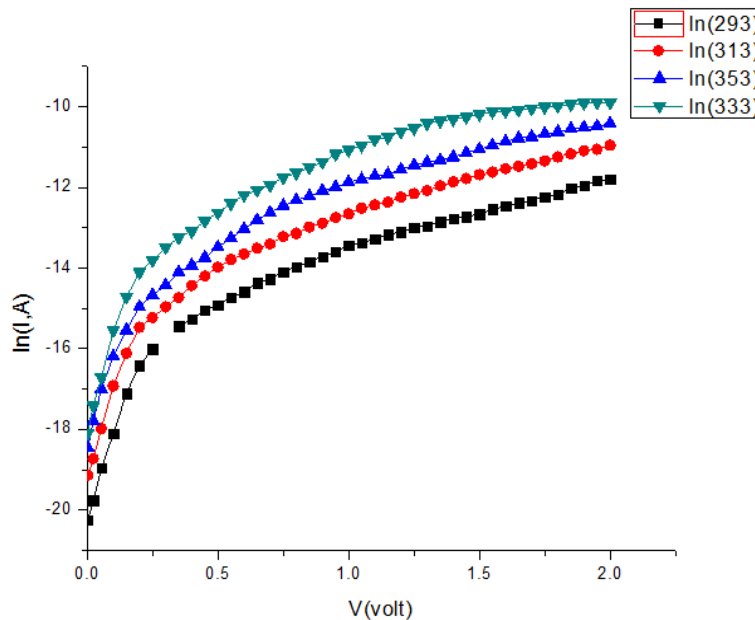


Fig.2-3 Dark I-V characteristics of CuTPP/p-Si/Al at different temperature in forward bias.

Fig.2-4 shows the ideality factor, m_1 , as a function of temperature, the figure indicated that the ideality factor decrease with increasing temperature in the range of temperature 293-353K. The values of m_1 are higher than unity which may be attributed to either recombination of free carriers in depletion region or the increase of diffusion current [29].

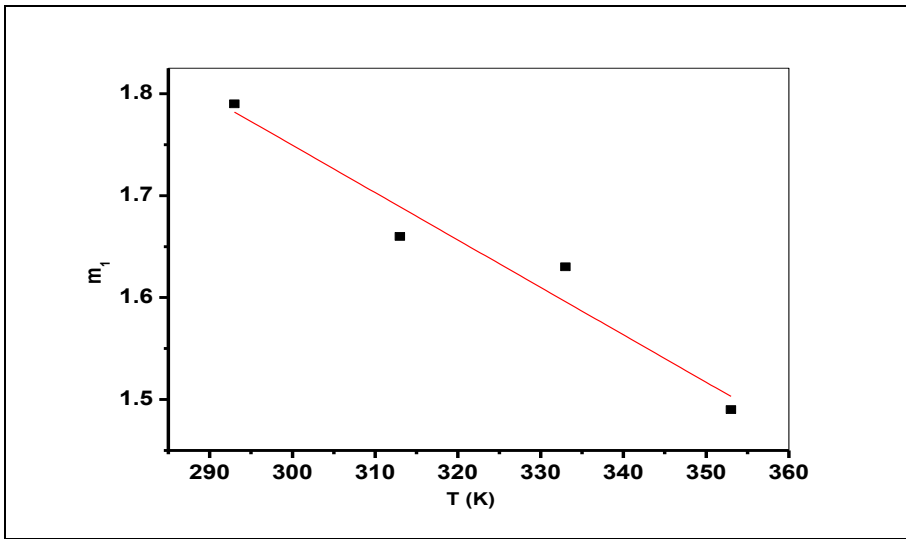


Fig.2-4 Temperature dependence of ideality factor, m_1 , for Au/CuTPP/p-Si/Al heterojunction device.

Fig.2-5 illustrates the $\ln(I)$ - $\ln(V)$ characteristics of Au/CuTPP/p-Si/Al heterojunction device for bias potentials greater than 0.3V. The slope of $\ln(I)$ - $\ln(V)$ plot is around 2 indicating that the space charge limited current (SCLC)

which single trap level conduction mechanism is the dominant conduction mechanism in that voltage range. The current density in this voltage range is controlled by equation (1.3) in chapter1.

Fig.2-5 shows the semi logarithms of forward current versus applied voltage at different temperature. This relation shows power law dependence with order ≈ 2 indicating that the SCLC with a single trap level is dominant in this voltage range.

The trapping factor θ' is defined by the ratio of free charge to trapped charge and is given by[30]:

$$\theta' = \frac{N_v}{N_t} \exp\left(\frac{-E_t}{k_B T}\right) \quad (2.3)$$

Where N_t is the total trap concentration at energy level E_t above the valence band edge and N_v is the effective density of states at the valence band edge.

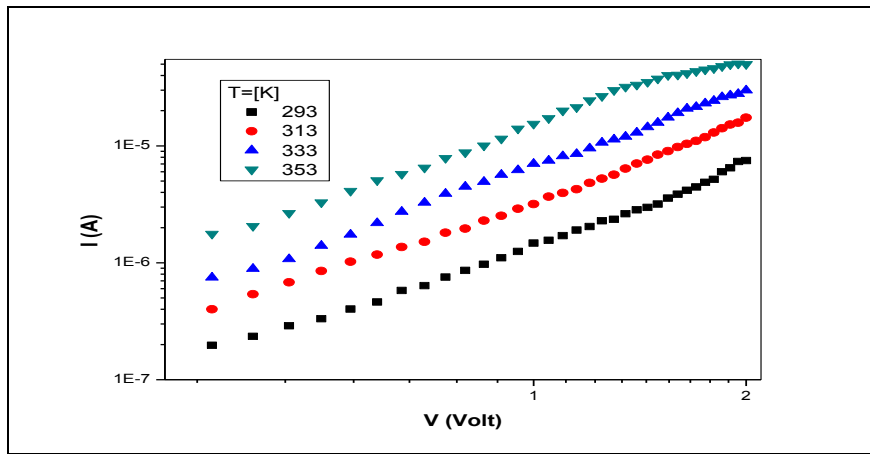


Fig.2-5 Variation of $\ln(I)$ with $\ln(V)$ for Au/CuTPP/p-Si/Al device for bias potentials greater than 0.3V.

Fig. 2-6 illustrates the temperature dependence of $\ln(I_f)$ in the space charge region. The trap level E_t is determined from the slope of the curves and has the value of 0.3 eV.

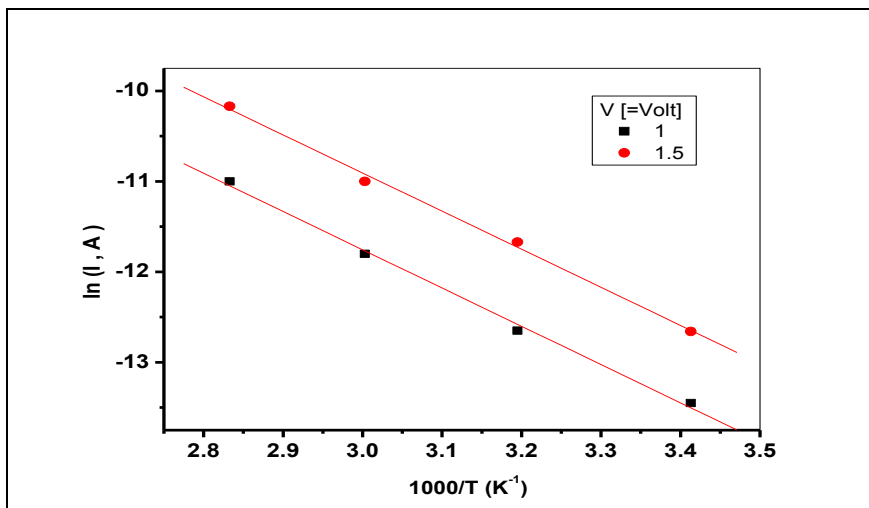


Fig.2-6 Variation of $\ln(I)$ with reciprocal temperature at forward bias potential of at 1 and 1.5 V.

2.2 Photovoltaic Properties:

Fig.2-7 illustrates the I-V characteristics of Au/CuTPP/p-Si/Al heterojunction solar cell measured at room temperature under illumination conditions. Under illumination, the light generates carrier-contribution photocurrent due to the production of electron-hole pairs. As it can be seen from Fig.2-7; the values of open circuit voltage (V_{oc}), short circuit current (I_{sc}), voltage at maximum power (V_M) and current at maximum power point (I_M) for the device are: 0.289V, 0.03mA, 0.16V and 0.022mA; respectively. The filling factor (FF) is given by $FF = V_M I_M / V_{oc} I_{sc}$. The calculated value of FF is 0.39. The experimental power conversion efficiency of a solar cell is given by:

$$\eta = FF V_{oc} I_{sc} / A P_{in} \quad (2.4)$$

where P_{in} is illumination intensity $\approx 5\text{mW/cm}^2$ and A is the effective area $= 2\text{mm}^2$. The calculated value of cell efficiency is 3.4%. The efficiency had been calculated without correcting for reflection or electrode absorption losses. The calculated parameters are in comparison to

other published heterojunction devices based on porphyrin molecule listed in Table 2.1.

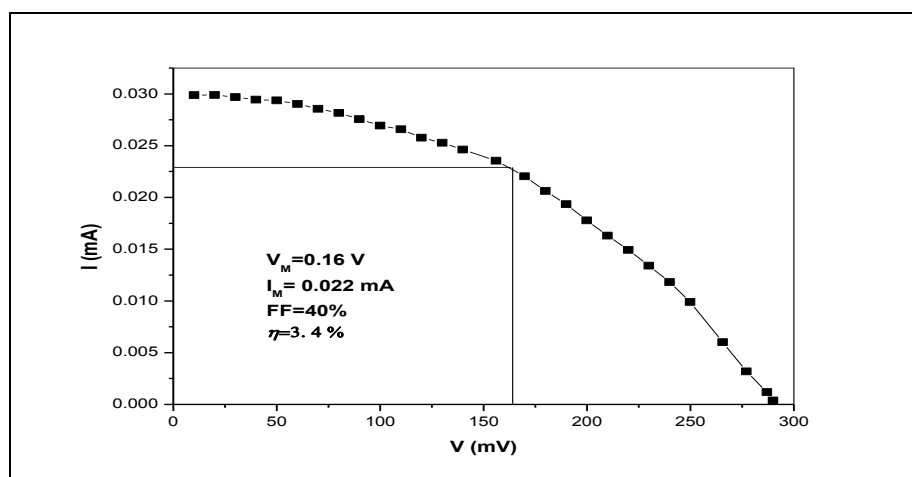


Fig.2-7 Current -voltage characteristics curve for Au/CuTPP/p-Si/Al heterojunction diode under illumination conditions at room temperature.

Table 2.1 Parameters of some organic solar cells based on porphyrin system.

Solar-cell construction	V_{oc} (V)	Fill Factor	Efficiency%	Ref.
Au/TPP/n-Si /Al	0.25	0.37	2.45	[6]
Au/FeTPP/Cl/p-Si/Al	0.47	0.32	5	[7]
Au/CuTPP/p-Si/Al	0.289	0.39	3.4	Present work

Conclusion

The Conclusion of this project showing that:

1-The values of the current increases as the temperature increase.

2-The dark current-voltage characteristics are extremely useful in identifying the operating transport conduction mechanisms.

3-In the first low voltage region $0 < V < 0.2$ Volt; the relation between $\ln(I)$ versus V is linear and the current of the Au/CuTPP/p-Si/Al device obeys the thermoionic emission of holes from p-Si substrate over the organic/inorganic barrier in the device.

4-the $\ln(I)$ - $\ln(V)$ characteristics of Au/CuTPP/p-Si/Al heterojunction device for bias potentials greater than 0.3V. The slope of $\ln(I)$ - $\ln(V)$ plot is around 2 indicating that the space charge limited current(SCLC) which single trap level conduction mechanism is the dominant conduction mechanism in that voltage range.

Reference:-

[1]H.Mifflin, The American Heritage Science Dictionary(2002).

[2]H.Lund, R.Nilsen, O.Salomatova, D.Skåre, E.Riisem (2008) .

[3]J.Allan, A.Paton, K.Turvey and D.Gerrad, Thermochemica Acta,143(1989)67.

[4] J.Nelson, Current Opinion in solid state and material science, 6(2002)87 .

[5] M.Aziz , Optical Materials , 3451(2008)1.

[6] M.El-Nahass, H.Metwally, H.El-Sayed and A.Hassanien, Synthetic Metals, 161 (2011) 2253.

[7] M.El-Nahass, H.Zeyada, M.Aziz and M.Makhlouf, Thin Solid Films, 492 (2005) 290.

[8] H.Zeyada, M.El-Nahass and M.Ali, Eur. Phys. J. Appl. Phys., 56(2011)10201.

[9] H.Zeyada, M.El-Nahass and M.Makhlouf, Current Applied Physics, 11 (2011) 1326.

[10] Nature Nanotechnology 4, 622 - 623 (2009).

[11] G.Chang, J.Forrest, E.Kurmaev, The paper " Oxygen-vacancy-induced ferromagnetism in undoped SbO₂ thin films" (2012)

[12] Haggard, Basics of Passive Solar Design,3(2008)22.

[13]<http://www.pveducation.org/pvcdrom/solar-cell-operation/solar-cell-structure>

- [14] M.Lampert and P.Mark, "Current Injection In Solid", Academic Press Inc, NewYourk, (1970).
- [15] M.Lampert, Rept. Progr. Phys., 27 (1964) 329.
- [16] G.Heilmeyer and G.Warfield, J. Chem. Phys., 38 (1963) 163.
- [17] M.Abkowitz, J.Facci and J.Rehm, J.Appl.Phys., 82(1998)2670.
- [18] M.Lampert, Rep. Prog. Phys., 27 (1964) 329.
- [19] R.Gould, Coordination Chemistry Reviews, 156 (1996) 237.
- [20] D.Rasmi, P.Battacharya, W.Perez, R.Katiyar and A.Bhalla, Appl. Phys. Lett., 81 (2002) 880.
- [21] W.Wang, T.Lee and M.Reed, Phys. Rev., 63 (2003) 35416.
- [22] P.Peumans and A.Yakimov, J.Appl. Phys., 93 (2003) 3693.
- [23] H.Hoppe and N.Sariciftci, J.Mater. Res., 19 (2004) 1924.
- [24] K.Mutolo, E.Mayo, B.Rand and S.Forrest, J.Am.Chem.Soc., 128 (2006)8108.
- [25] S.Gledhill, B.Scott and B.Gregg, J. Mater. Res, 20 (2005) 3167.
- [26] I.D. Parker, J. Appl. Phys, 75(1994)1656.
- [27] S. Riad, Thin Solid Films, 370 (2000) 253.

[28] D.Morgan, Y.Aliyu and R.Bunce, Phys. Status Solidi, 133(1992)77.

[29] T.Shafai and T.Anthopoulos, Thin Solid Films, 398(2001)361.

[30] M.Lampert, Rep. Prog. Phys., 27 (1964) 329.